

## ARTICLES

**Magnetostructural effects and phase transition in Cr<sub>2</sub>O<sub>3</sub> under pressure**

Alexander Yu. Dobin, Wenhui Duan, and Renata M. Wentzcovitch

*Department of Chemical Engineering and Material Sciences, School of Physics and Astronomy, and Minnesota Supercomputer Institute, University of Minnesota, Minneapolis, Minnesota 55455*

(Received 9 March 2000)

We have successfully calculated the electronic and structural properties of chromia (Cr<sub>2</sub>O<sub>3</sub>) in the local spin density approximation. We predict a transformation from the corundum to the Rh<sub>2</sub>O<sub>3</sub> (II) structure around 15 GPa in the antiferromagnetic (AFM) phase as well as in the paramagnetic (PM) insulating state which occurs above the Néel temperature ( $T_N$ ). This transition is relevant to interpreting the optical anomalies observed in the absorption spectrum of ruby under pressure. We have modeled the structural properties of the PM state using a Landau-like expansion of the magnetostriction energy. This treatment correctly describes the structural anomalies across  $T_N$  in the corundum phase and indicates that the AFM and PM insulating states should have distinct compressive behaviors.

Oxides of the 3d transition metals are a fascinating class of materials with amazingly diverse physical properties. They have been the subject of intensive experimental and theoretical studies for many years.<sup>1-4</sup> A wide variety of computational techniques — density-functional theory with the linear augmented plane-wave method,<sup>2,5</sup> nonperiodic embedded cluster approach,<sup>6,7</sup> and periodic unrestricted Hartree-Fock method<sup>8,9</sup> — have been used to perform *ab initio* calculations of these compounds. In this paper we report a successful application of the first-principles pseudopotential plane-wave (PPPW) approach<sup>10</sup> to compute the structural properties of and predict a pressure-induced structural transition in chromia (Cr<sub>2</sub>O<sub>3</sub>), a typical antiferromagnetic (AFM) insulator in this class of materials. There have been a few experimental papers on chromia<sup>11-14</sup> and only one *ab initio* calculation.<sup>9</sup> The periodic unrestricted linear combination of atomic orbitals (LCAO) Hartree-Fock method was used<sup>9</sup> to calculate crystal parameters and elastic properties, as well as electronic structure of Cr<sub>2</sub>O<sub>3</sub>. Their results are in a good agreement with experimental data. The advantage of the PPPW approach is in the simplicity of the plane-wave basis set, which makes it easy to calculate ionic forces and lattice stresses. This allowed us to optimize dynamically the cell structure of chromia under pressure<sup>15</sup> for various magnetic states.

Our motivation to study Cr<sub>2</sub>O<sub>3</sub> is related to the high-pressure behavior of ruby, i.e., Al<sub>2(1-x)</sub>Cr<sub>2x</sub>O<sub>3</sub> ( $x < 0.05$ ). The pressure dependence of the fluorescence lines in ruby is widely used to determine pressure (the so-called ruby scale) in diamond-anvil-cell experiments. Alumina (Al<sub>2</sub>O<sub>3</sub>) and chromia exist in the corundum phase and form a completely isomorphous alloy system. Alumina has been shown to undergo a structural phase transition to the Rh<sub>2</sub>O<sub>3</sub> (II) phase around 80–100 GPa.<sup>16-18</sup> A recent theoretical study<sup>19</sup> of the effect of this structural transition on the optical spectrum of ruby indicated that the neighborhood of the chromium site, a *color center*, might be undergoing a severe distortion around 30 GPa. This hypothesis is suggested by the behavior of the optical absorption lines which display a small discontinuity

at 30 GPa and resemble more closely the transitions predicted in the high-pressure Rh<sub>2</sub>O<sub>3</sub> (II) phase beyond 30 GPa than those in the corundum phase. It was then anticipated that the cause of this distortion could be a similar phase transformation at lower pressures (<30 GPa) in chromia, the other end member of the alloy. At the moment there is no convincing experimental evidence for a phase transformation in Cr<sub>2</sub>O<sub>3</sub> in this pressure range.<sup>20</sup> However, this may be due to the fact that the Rh<sub>2</sub>O<sub>3</sub> (II) phase has an x-ray diffraction pattern similar to corundum's,<sup>16</sup> which makes it difficult to observe.

In this paper we investigate this pressure-induced transformation in chromia. However, another interesting question arises: at room temperature chromia undergoes a change in magnetic phase under pressure. Its Néel temperature is  $T_N = 308$  K,<sup>21</sup> with a pressure dependence of  $\partial T_N / \partial P = -16$  K/GPa.<sup>22</sup> The paramagnetic (PM) state above  $T_N$  is also insulating; therefore, the effects of the magnetic transition on the structural properties are not expected to be dramatic. Nevertheless, structural anomalies around the Néel temperature are well known<sup>23,24</sup> and a realistic prediction of a possible phase transition above 0.5 GPa should be carried out in the PM insulating phase with randomly oriented spins. Here we investigate from first principles this structural transition in the AFM and in a hypothetical ferromagnetic (FM) phase. The structural properties of the PM insulating state are then explored in relation to those of the AFM and FM phases using a phenomenological approach based on a Landau-like expansion of the magnetostriction energy. The predicted structural differences of this phase with respect to the AFM phase correlate well with the anomalies observed around the Néel transition and are very different from those of the PM metallic phase predicted by a standard local density approximation (LDA) calculation.

The crystal structure of Cr<sub>2</sub>O<sub>3</sub> at ambient conditions is corundum like. It can be described as a hexagonal close-packed array of oxygens with two-thirds of the octahedral sites filled with chromium atoms. The unit cell is rhombohedral and contains two formula units. In Cr<sub>2</sub>O<sub>3</sub> each chro-

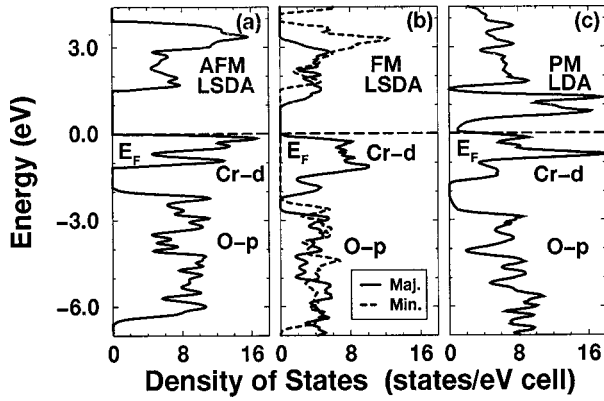


FIG. 1. Calculated density of states (DOS) for various magnetic phases of  $\text{Cr}_2\text{O}_3$  in the corundum structure.

mium is left with three  $d$  electrons, losing the other three to oxygen atoms. The predominantly octahedral crystal field splits the  $d$  orbitals into (approximately) a  $t_{2g}$ -like triplet and an  $e_g$ -like doublet. The lower triplet accommodates three electrons. The  $\text{Cr}^{3+}$  local magnetic moment is  $2.76\mu_B$ ,<sup>21</sup> close to the spin-only value of  $3\mu_B$ . The moments alternate up and down along the  $c$  axis. In the insulating phase above  $T_N$  chromia has randomly oriented spins.

To investigate the effect of magnetism on the structural properties we have performed three distinct calculations: (1) a standard *spin-polarized* local spin density approximation (LSDA) calculation<sup>25</sup> in the AFM phase of  $\text{Cr}_2\text{O}_3$  in the corundum structure, (2) the same type of calculation in the FM phase, with the net magnetic moment of  $3\mu_B$  per Cr atom, and (3) a standard *non-spin-polarized* LDA calculation in a PM phase. In all cases the lattice and internal degrees of freedom were dynamically relaxed under pressure.<sup>15</sup> The zero-pressure structures obtained correspond to various local minima of the LSD functional.

The ground state at  $T=0$  K is the AFM state with a band gap of  $\approx 1.5$  eV [Fig. 1(a)] and a local magnetic moment of  $3\mu_B$  on chromium atoms (from straight band occupations). The overall band structure compares well with photoemission data.<sup>29,30</sup> Namely, the  $\text{O}_{2p}$  and  $\text{Cr}_{3d}$  bandwidths of 5 eV and 1 eV, respectively, and  $\text{O}_{2p}$ - $\text{Cr}_{3d}$  band center separation of 4 eV are in a good agreement with experimental values. However, as expected, the band gap is underestimated with respect to the thermal gap of 3.3 eV.<sup>31</sup> Zero-pressure equilibrium structural parameters presented in Table I are also in good agreement with experimental data. The cohesive energy of  $E_{coh}=6.1$  eV/atom compares well with  $E_{coh}=5.55$  eV/atom from experiments. The FM state is found to be insulating as well with a band gap of  $\approx 0.9$  eV [Fig. 1(b)]. After structural relaxation this state is only 35 meV/unit above the AFM ground state. The equilibrium lattice parameters (Table I) are quite different from those in the AFM state, indicating a substantial influence of the magnetic state on the structural properties. The standard paramagnetic *non-spin-polarized* LDA calculation stabilizes  $\text{Cr}_2\text{O}_3$  in a *metallic* phase [Fig. 1(c)], as expected, with structural properties considerably different from the observed ones (see Table I). This state is 2.25 eV/unit above the AFM ground state and cannot properly account for the structural transition under consideration.

Our description of the structural properties of the PM

TABLE I. Zero-pressure structural parameters of chromia in the corundum structure (rhombohedral unit cell): lattice constant  $a_0$  ( $\text{\AA}$ ) and rhombohedral angle  $\alpha$  (deg), internal atomic coordinates  $u(\text{Cr})$  and  $u(\text{O})$ , bulk modulus  $B_0$  (GPa), and its pressure derivative  $B'_0$ .

	AFM LSDA	FM LSDA	PM LDA	Experiment
$a_0$	5.366	5.308	5.688	$5.362^c$ $5.350^d$
$\alpha$	55.17	56.14	47.23	$55.108^c$ $55.128^d$
$u(\text{Cr})$	0.347	0.351	0.337	$0.3475^c$ $0.3477^d$
$u(\text{O})$	0.557	0.550	0.583	$0.556^c$ $0.555^d$
$B_0^a$	$251 \pm 6$	$215 \pm 5$	$300 \pm 8$	$238 \pm 4^d$ $222 \pm 2^f$
$B_0^b$	$261 \pm 2$	$211 \pm 5$	$297 \pm 3$	$231 \pm 5^f$
$B'_0^b$	2.59	2.73	4.24	$2.0 \pm 1.1^f$

<sup>a</sup>Second-order finite strain equation of state (FSEOS) ( $B'_0=4$ ). We used our data up to 15 GPa for this fitting.

<sup>b</sup>Third-order FSEOS was used with  $B'_0$  as a free parameter. We include pressures up to 140 GPa to get a correct value of  $B'_0$ , while in Ref. 12 the pressure range was not sufficient for a confident determination of  $B'_0$ .

<sup>c</sup>Reference 11.

<sup>d</sup>Reference 13.

<sup>e</sup>Reference 12.

phase is based on the Landau-like expansion of the crystal deformation energy at a certain fixed pressure,  $E = \lambda_{ikjl}u_{ik}u_{jl} + \beta_{ikjl}u_{ik}M_{1j}M_{2l}$ . Here  $u_{ik}$  is a strain tensor,  $\mathbf{M}_1$ ,  $\mathbf{M}_2$  are the magnetization vectors of the two AFM sublattices, and  $\lambda$  and  $\beta$  are constant tensors. The first term represents pure elastic deformation, while the second describes the magnetostriction energy, i.e., the coupling of the magnetic and structural degrees of freedom. Deformations conserving the corundum structure symmetry allow only for  $U = u_{33}$ , uniaxial strain, and  $V = \sum u_{ii}$ , hydrostatic compression. We assume  $\mathbf{M}_1$ ,  $\mathbf{M}_2$  remain parallel to the  $z$  axis. The above expression then simplifies to  $E = \lambda_1 V^2 + \lambda_2 U^2 - \lambda_{12} V U + (\beta_1 V + \beta_2 U) M_{1z} M_{2z}$ . The equilibrium configurations are such that  $U = u_0 M_{1z} M_{2z}$ ,  $V = v_0 M_{1z} M_{2z}$ , where  $u_0$  and  $v_0$  depend on  $\lambda$  and  $\beta$ . For the AFM and FM phases  $M_{1z} M_{2z} = -1$  and  $M_{1z} M_{2z} = 1$ , respectively. For the PM state the average product  $\langle M_{1z} M_{2z} \rangle_{PM} = 0$ . Therefore, the equilibrium lattice structural parameters of the PM phase are given by  $U_{PM} = (U_{AFM} + U_{FM})/2$ ,  $V_{PM} = (V_{AFM} + V_{FM})/2$  where  $U_{AFM}$ ,  $U_{FM}$ ,  $V_{AFM}$ , and  $V_{FM}$  have been determined from first principles. A similar procedure can be adopted for dealing with the  $\text{Rh}_2\text{O}_3$  (II) phase. In this case, the deformation energy is expressed as  $E = \sum \lambda_{\gamma\delta} u_{\gamma} u_{\delta} + \sum \beta_{\gamma\mu} u_{\gamma} M_{1z} M_{2z}$ , where  $\gamma, \delta = xx, yy, zz$ .

The predicted properties of the AFM and PM insulating states compare as follows: (a) the differences in zero-pressure lattice parameters (in the hexagonal cell description) between them are similar to the anomalies observed around  $T_N$ . Throughout the Néel transition (AFM to PM), the calculated  $\Delta a_H = +0.013$   $\text{\AA}$  and  $\Delta c_H = -0.11$   $\text{\AA}$  agree in sign and approximately in order of magnitude with the experimental values of  $\Delta a_H = +0.006$   $\text{\AA}$  and  $\Delta c_H = -0.018$   $\text{\AA}$ .<sup>23</sup> We believe that this is evidence of the satisfactory description of the PM insulating state. (b) The calculated compressive behavior of our PM insulating state compares well with the experimental behavior under pressure above  $T_N$ ,<sup>12</sup> while our AFM calculation is in better agreement with the experi-

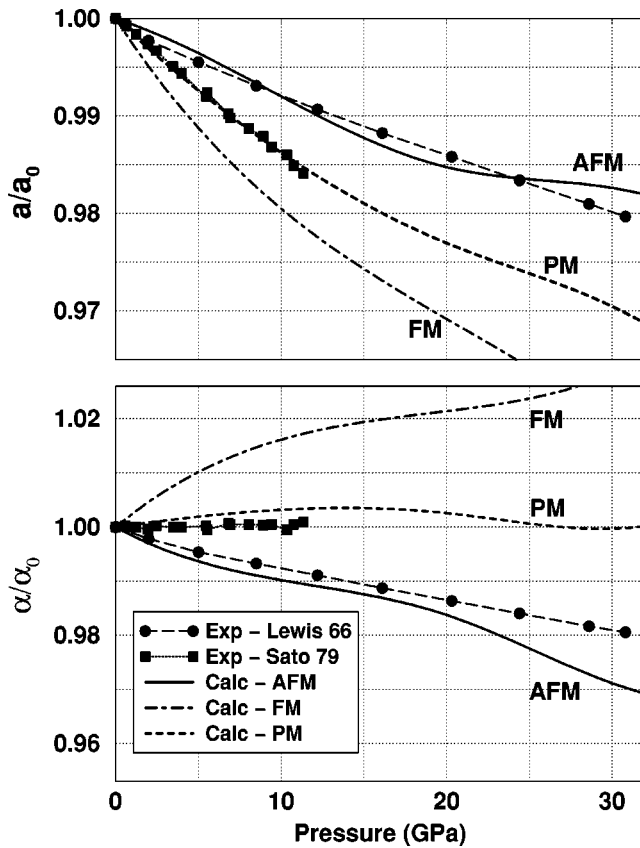


FIG. 2. Pressure dependence of the  $\text{Cr}_2\text{O}_3$  rhombohedral cell constant  $a$  and angle  $\alpha$ , calculated for the AFM, FM, and PM phases compared to experimental measurements from Ref. 11 (Lewis 66) and Ref. 12 (Sato 79).

ment of Lewis and Drickamer,<sup>11</sup> which we suspect may have been carried out in the AFM phase.

A summary of experimental data and our results is presented in Fig. 2. In Ref. 11 a substantial decrease of the rhombohedral angle with pressure was found (hexagonal  $c$  axis less compressive than the  $a$ - $b$  axes). In contrast, in Ref. 12 a slight increase in this angle was observed ( $c$  axis more compressive than the  $a$ - $b$  axes). This discrepancy has been attributed to nonhydrostatic stresses in Ref. 11. Our results suggest that this discrepancy could be real if somehow in Ref. 11 chromia was kept in the AFM state. We predict here that the magnetic state affects noticeably the compressive behavior of chromia despite the insulating nature of both phases. Compression experiments well below and well above  $T_N$  could help to clarify this situation.

Now we deal with the structural transition. The high-pressure  $\text{Rh}_2\text{O}_3$  (II) phase has the  $Pbna$  space group with an orthorhombic unit cell containing 20 atoms (four  $\text{Cr}_2\text{O}_3$  units). This phase is structurally similar to the corundum structure and may be described as having a different stacking of similar octahedral layers with a periodicity which is twice that of the corundum along the  $c$  direction.<sup>32</sup> In the corundum structure the  $\text{CrO}_6$  octahedra share three edges while in the  $\text{Rh}_2\text{O}_3$  (II) structure they share only two. The relative stability of these structures in both magnetic states is shown in Fig. 3(a). We predict the corundum to  $\text{Rh}_2\text{O}_3$  (II) transformation in chromia to take place at 14 GPa and 16 GPa in the AFM and in the PM insulating phases, respectively, with

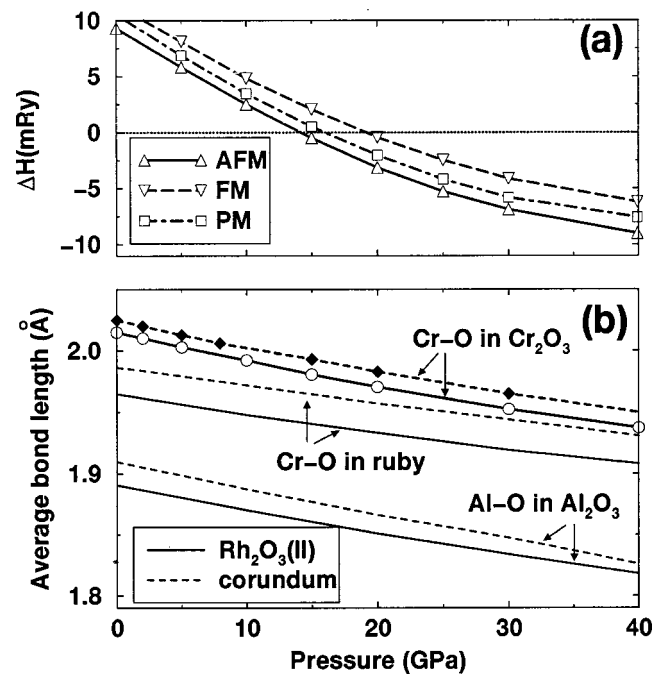


FIG. 3. (a) Pressure dependence of the enthalpy for  $\text{Rh}_2\text{O}_3$  (II) structure, relative to the corundum in the AFM and PM phases; (b) average radii of the first coordination shell around chromium in chromia and ruby (Ref. 19), and aluminum in alumina (Ref. 19).

fractional volume changes at the transition of  $\approx -2\%$ . This transition would also take place in the FM phase if it were somehow stabilized.

Figure 3(b) displays the average radius of the first coordination shell around chromium in AFM chromia and in ruby (from Ref. 19). The average Cr-O bond length in chromia increases across the corundum to  $\text{Rh}_2\text{O}_3$  (II) transition by an amount similar to that required to explain the optical anomalies in ruby under pressure, which can be explained by a decrease in crystal field splitting. This verifies that this presumable rearrangement could arise from a preference of chromia for the  $\text{Rh}_2\text{O}_3$  (II) phase above  $\approx 15$  GPa. The structural constraint imposed by the alumina host structure should naturally hinder the atomic rearrangement around the color centers until higher pressures, for instance, 30 GPa.

These results should stimulate further experimental and theoretical work. The prediction of distinct compressive behaviors in chromia above and below  $T_N$  and the structural phase transformation near 15 GPa await experimental confirmations. The latter, if verified, makes ruby an interesting study case: an isomorphous alloy in which both end members undergo the same structural transition but at very different pressures. Intermediate compositions should undergo similar transitions at intermediate pressures. However, before the transformation manifests macroscopically it could be nucleating around one of the components, even in the impurity limit. The possibility of investigating this phenomenon in ruby by extended x-ray absorption fine structure (EXAFS) or anomalous x-ray scattering is fascinating.

We thank Phil Allen and Stefano Baroni for helpful comments on the manuscript. This work was supported by the University of Minnesota MRSEC (A.Yu.D.) and NSF Grant No. EAR-9973130 (R.M.W. and W.D.).

- <sup>1</sup>N.F. Mott, Proc. Phys. Soc., London, Sect. A **68**, 416 (1949); J. Hubbard, *ibid.* **277**, 237 (1964); **5**, 401 (1964); B.H. Brandow, Adv. Phys. **26**, 651 (1977).
- <sup>2</sup>K. Terakura *et al.*, Phys. Rev. Lett. **52**, 1830 (1984); Phys. Rev. B **30**, 4734 (1984).
- <sup>3</sup>R.M. Wentzcovitch, W. Schulz, and P.B. Allen, Phys. Rev. Lett. **72**, 3389 (1993); **73**, 3043 (1994).
- <sup>4</sup>S.P. Lewis, P.B. Allen, and T. Sasaki, Phys. Rev. B **55**, 10 253 (1997).
- <sup>5</sup>P. Dufek *et al.*, Phys. Rev. B **49**, 10 170 (1994).
- <sup>6</sup>J. Casanovas and F. Illas, Phys. Rev. B **50**, 3789 (1994).
- <sup>7</sup>J.A. Mejias and J.F. Sanz, J. Chem. Phys. **102**, 850 (1995).
- <sup>8</sup>M.D. Towler *et al.*, Phys. Rev. B **50**, 5041 (1994).
- <sup>9</sup>M. Catti *et al.*, J. Phys. Chem. Solids **57**, 1735 (1996).
- <sup>10</sup>M.L. Cohen, Phys. Scr. **T1**, 5 (1982); W.E. Pickett, Comput. Phys. Rep. **9**, 115 (1989).
- <sup>11</sup>G.K. Lewis, Jr. and H.G. Drickamer, J. Chem. Phys. **45**, 224 (1966).
- <sup>12</sup>Y. Sato and S. Akimoto, J. Appl. Phys. **50**, 5285 (1979).
- <sup>13</sup>L.W. Finger and R.M. Hazen, J. Appl. Phys. **51**, 5362 (1980).
- <sup>14</sup>X. Li, L. Liu, and V.E. Henrich, Solid State Commun. **84**, 1103 (1992).
- <sup>15</sup>R.M. Wentzcovitch, J.L. Martins, and G.D. Price, Phys. Rev. Lett. **70**, 3947 (1993).
- <sup>16</sup>K.T. Thomson, R.M. Wentzcovitch, and M.S.T. Bukowinski, Science **274**, 1880 (1996).
- <sup>17</sup>H. Cynn *et al.*, Am. Mineral. **75**, 439 (1990); F.C. Marton and R.E. Cohen, *ibid.* **79**, 789 (1994).
- <sup>18</sup>N. Funamori and R. Jeanloz, Science **278**, 1109 (1997).
- <sup>19</sup>W. Duan *et al.*, Phys. Rev. Lett. **81**, 3267 (1998).
- <sup>20</sup>L.-G. Liu and W. A. Bassett, *Elements, Oxides, and Silicates: High Pressure Phases with Implications for the Earth's Interior* (Oxford Press, New York, 1986), p. 126.
- <sup>21</sup>L.M. Corliss *et al.*, J. Appl. Phys. **36**, 1099 (1965).
- <sup>22</sup>T.G. Worlton, R.M. Brugger, and R.B. Bennion, J. Phys. Chem. Solids **29**, 435 (1968).
- <sup>23</sup>H.L. Alberts and J.C.A. Boeyens, J. Magn. Magn. Mater. **2**, 327 (1976). Lattice parameters in the PM phase were measured up to  $T=400$  K and extrapolated to  $T=0$  K.
- <sup>24</sup>S. Greenwald, Nature (London) **177**, 286 (1956).
- <sup>25</sup>The norm-conserving Troullier-Martins (Ref. 26) pseudopotentials (cutoff radii in a.u.: O,  $r_s=r_p=1.45$ ; Cr,  $r_s=r_p=2.5$ ,  $r_d=1.75$ ) with partial core correction (Ref. 27) (pseudocore radius for Cr:  $r_c=1.6$ ) in the plane-wave basis set were used (Ref. 10). The plane-wave energy cutoffs were 70 Ry for wave functions and 280 Ry for charge densities and potentials. Brillouin-zone summations were performed over two  $k$  points in the irreducible wedge. We used the Ceperley-Alder LSDA exchange-correlation potential parametrized by Perdew and Zunger (Ref. 28).
- <sup>26</sup>N. Troullier and J.L. Martins, Phys. Rev. B **43**, 1993 (1991).
- <sup>27</sup>S.G. Louie, S. Froyen, and M.L. Cohen, Phys. Rev. B **26**, 1738 (1982).
- <sup>28</sup>D.M. Ceperley and B.J. Alder, Phys. Rev. Lett. **45**, 566 (1980); J.P. Perdew and A. Zunger, Phys. Rev. B **23**, 5048 (1981).
- <sup>29</sup>G.K. Wertheim, H.J. Guggenheim, and S. Hüfner, Phys. Rev. Lett. **30**, 1050 (1973).
- <sup>30</sup>D.E. Eastman and J.L. Freeouf, Phys. Rev. Lett. **34**, 395 (1975).
- <sup>31</sup>J.A. Crawford and R.W. Vest, J. Appl. Phys. **35**, 2413 (1964).
- <sup>32</sup>R.D. Shannon and C.T. Prewitt, J. Solid State Chem. **2**, 134 (1970).